

Equatorial twists to mid-latitude dynamics

As we saw for Stommel's or Munk's wind-driven gyres and for Sverdrup's balance, there was no particular problem with the equator. In fact, Stommel solved his gyre for no rotation of the earth at all. But we do need to return to the barotropic potential vorticity balance and discuss one aspect (involving linearization) that is different in equatorial dynamics.

The wind-driven models of Stommel and Munk employed a linearization involving a small parameter, the Rossby number, which we need to reconsider. Recall

$$f \approx [f]$$

$$\zeta \approx [u / L]$$

$$h \approx [h]$$

$$H \approx [H_0]$$

$$\left[\frac{f + \zeta}{H + h} \right] \approx \left[\frac{f}{H_0} \right] \left[\frac{1 + (u / fL)}{1 + (h / H_0)} \right] \approx \left[\frac{f}{H_0} \right], \text{ if}$$

$$R \equiv [u / fL] \ll 1, \text{ and } [h / H_0] \ll 1$$

Clearly near the equator, f becomes arbitrarily small and this definition of the Rossby number leads one to suspect that the flow cannot be linear.

However, we can fix this by recognizing that for steady flows:

$$f = \beta y; f_y \approx [\beta]$$

$$\zeta_{x,y} \approx [u / L]$$

$$\frac{d}{dt} [f + \zeta] = v\beta + (u\zeta_x + v\zeta_y) \approx [\beta u] [1 + (u / \beta L^2)]$$

$$\frac{d}{dt} \left[\frac{f + \zeta}{H + h} \right] \approx \left[\frac{\beta u}{H_0} \right] \left[\frac{1 + (u / \beta L^2)}{1 + (h / H_0)} \right] \approx \left[\frac{\beta u}{H_0} \right], \text{ if}$$

$$R_E \equiv [u / \beta L^2] \ll 1, \text{ and } [h / H_0] \ll 1$$

For equatorial dynamics a new parameter R_E must be small for the flow to be linear in the same sense as for mid-latitudes. This is somewhat less stringent than for mid-latitudes. Try putting some values into the two different

“Rossby” numbers and see which one is larger. Recall the definition of β . At the equator it has a value of approximately $2 \times 10^{-11} \text{ (ms)}^{-1}$.

The equations of motion near the equator can be written using the equatorial β -plane as follows:

$$\frac{du}{dt} - \beta y v = -\frac{1}{\rho} \frac{\partial p}{\partial x} - r u + \frac{\tau_z^x}{\rho},$$

$$\frac{dv}{dt} + \beta y u = -\frac{1}{\rho} \frac{\partial p}{\partial y} - r v + \frac{\tau_z^y}{\rho}$$

$$0 = -\frac{1}{\rho} \frac{\partial p}{\partial z} - g,$$

$$\frac{\partial u}{\partial x} + \frac{\partial v}{\partial y} + \frac{\partial w}{\partial z} = 0,$$

$$\frac{d}{dt} \equiv \frac{\partial}{\partial t} + u \frac{\partial}{\partial x} + v \frac{\partial}{\partial y} + w \frac{\partial}{\partial z}$$

Steady, linear flow near the equator demands that terms with (d/dt) are set to zero. The first two equations then reduce to the following:

$$\begin{aligned} -\beta y v &= -\frac{1}{\rho} \frac{\partial p}{\partial x} - r u + \frac{\tau_z^x}{\rho} \\ +\beta y u &= -\frac{1}{\rho} \frac{\partial p}{\partial y} - r v + \frac{\tau_z^y}{\rho} \end{aligned}$$

At the equator, the left hand sides of both of the above must vanish. This results in a balance in which very near the surface, where the pressure gradient is small, the currents are down-wind. Where the pressure gradient is larger than the wind forcing, the currents are then down-pressure gradient. While Stommel (1960, DSR) seems to have been the only one to explore this for the case in which the wind stress is zonal and uniform with latitude, this balance lies at the heart of the description of surface and subsurface flows at the equator, and the simplified explanation for the equatorial undercurrent (EUC) in *Ocean Circulation*. We will look further along these lines shortly.

The EUC occurs at a depth where horizontal pressure gradients (higher pressure on western sides of the basins due to westward wind stress at the surface piling up water) drive an eastward flow at depth. It also can apply to the meridional (north/south) flows: at the surface, where wind stress is blowing to the north across the equator, there is a surface flow in the direction of the wind (South Equatorial Current, SEC), but at depth, pressure gradients may drive an opposing flow to the south. Indeed, there is evidence for mean meridional slopes of the sea surface across the equator, with generally higher sea surface height to the north as a consequence of positive meridional wind stress at the equator. Recall that the ITCZ is, in the mean, located to the north of the equator.

The second equation above has been used to calculate a geostrophic zonal velocity AT the equator. (Jerlov, 1953, Tellus) was the first explore this balance. It can be most simply stated by neglecting the effects of friction (proportional to r) as follows.

Let $u = u^g + u^f$. In the second momentum equation above, we now have

$$+ \rho\beta y(u^g + u^f) = -p_y + \tau_z^y$$

If we take the “y” derivative of both sides of the above and evaluate it at the equator ($y=0$), this equation becomes

$$+ \rho\beta u^g = -p_{yy}$$

$$+ \rho\beta u^f = +\tau_{yz}^y$$

This balance assumes that

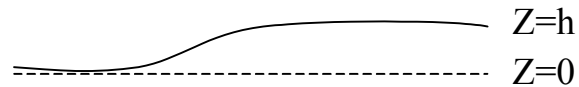
$$0 = -p_y + \tau_z^y$$

and that u_y is finite. The first of these three equations is often used to calculate “geostrophic” flow at the equator, but the additional two constraints are usually ignored. This is discussed further by Joyce (right, that’s me!, 1988, JPO). A recent (as yet unpublished) study of Sverdrup dynamics in the equatorial Pacific by Kessler can be found on the web at <http://www.pmel.noaa.gov/~kessler/kjm01-abstract.html>

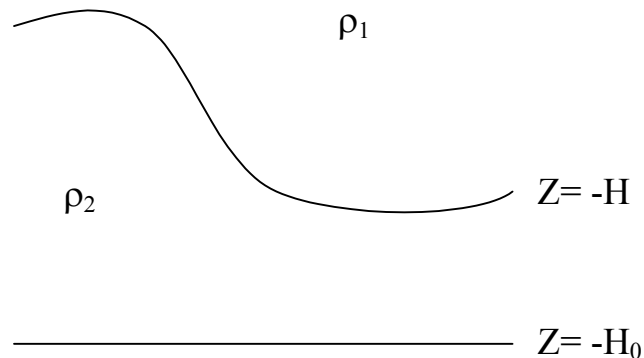
Equatorial Dynamics 101

To examine the zonal momentum balances at the equator, we will use the simplified dynamics contained in

$$0 = -p_x + \tau_z^x$$



Consider the figure at the right, which we already have used in previous notes. If we think of ourselves looking at the equatorial Pacific Ocean (for example) from a point in the northern hemisphere, the sea surface slopes upwards to the west under the trades and the pycnocline underneath slopes oppositely so as to make for no



or reduced pressure gradients at depth. In the upper layer, which can be in motion, we have $p_x = \rho_1 g h_x$. This is constant throughout the upper layer since the density is assumed constant. If we integrate the above equation from the free surface to a depth z within the upper layer, we obtain

$$0 = -\rho_1 g (h - z) h_x + \tau^x(z = h) - \tau^x(z), \text{ but}$$

$$\tau^x(z) = r(z)u(z), \text{ where } r(z) \text{ is the friction parameter, thus}$$

$$r(z)u(z) = \tau^x(z = h) - \rho_1 g (h - z) h_x$$

If we knew something about $r(z)$, we could solve for the zonal current variation with depth using the last of the equations above. Near the surface ($z=h$), the second term on the right of the last equation is small and the flow is in the direction of the surface stress (to the west since $\tau^x(h)$ is negative on the equator). This is the westward SEC. In this simple model, the vertical integral of the zonal flow must vanish since there is no source for inflow from the sides or thru the bottom of the upper layer. Near the bottom of the upper layer, $r(z)$ becomes small, z approaches $-H$, the second term on the right is larger than the first and the flow becomes positive (and possibly large). This is the EUC. The depth of no zonal flow (between the SEC and

EUC), called ($z=z_0$) can be written down without knowledge of the friction parameter.

$$0 = r(z_0)u(z_0) = \tau^x(z = z_0) - \rho_1 g(h - z_0)h_x, \text{ or}$$

It is merely the depth where the surface stress exactly balances the horizontal pressure gradient. This can be solved for z_0 and estimated readily from data. As you will recall from an earlier discussion, the variation of surface elevation h is much smaller than that of the upper layer depth H by a factor of $\Delta\rho/\rho$. So we could also simplify the above even more by replacing $\rho_1 h_x$ by $\Delta\rho H_x$ and using a figure such as fig. 5.4 (p. 148 of 2nd ed. textbook). Let's try putting in some numbers and seeing what we get. From the above, we can solve for z_0 .

$$z_0 \approx -\tau^x(z = z_0) / gh_x, \text{ for } |h/z_0| \ll 1,$$

$$\tau^x \sim -0.04 \text{ nt} / \text{m}^2,$$

$$h_x \sim -0.5\text{m} / 9000\text{km} = -0.56 \cdot 10^{-6}, \text{ thus}$$

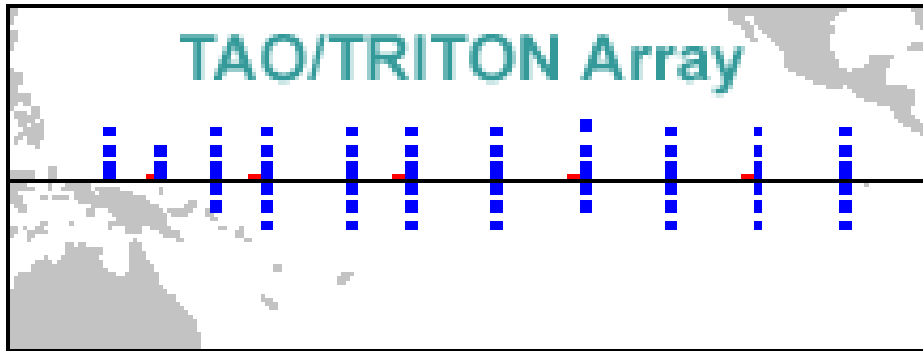
$$z_0 \approx -74\text{m},$$

which is indeed much larger in magnitude than the sea surface elevation. This depth separates the westward flowing South Equatorial Current on the equator from the eastward flowing Equatorial Undercurrent. It is not a bad estimate looking at the upper panel of fig. 5.5 in the text.

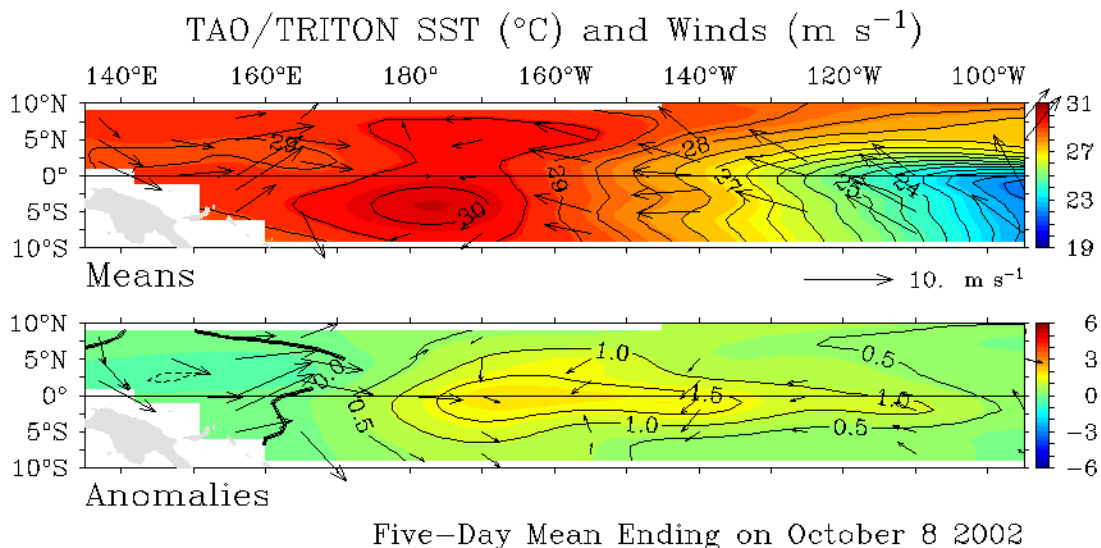
Observations of the Equatorial Ocean

Because of the legacy of the Tropical Ocean, Global Atmosphere (TOGA) Program, we have learned a great deal about equatorial dynamics and the reasons for changes in the equatorial circulation. One such change, in which the trades weaken significantly across the Pacific Ocean, the thermocline slope is greatly reduced from west to east, and the upwelling of cold water in the eastern Pacific Ocean is terminated, is something called El Niño. This is discussed in the text. Because of the demonstrated human dimension of these changes, mainly due to changes in tropical precipitation, a real time monitoring system has been maintained in the tropical Pacific with data employed in some predictive models of equatorial dynamics than can be

used to forecast the occurrence of El Niño and its opposite extreme, La Niña. Access to these data can be found on the web at: <http://www.pmel.noaa.gov/tao/> . An array of moorings is in place in the Pacific as shown below:

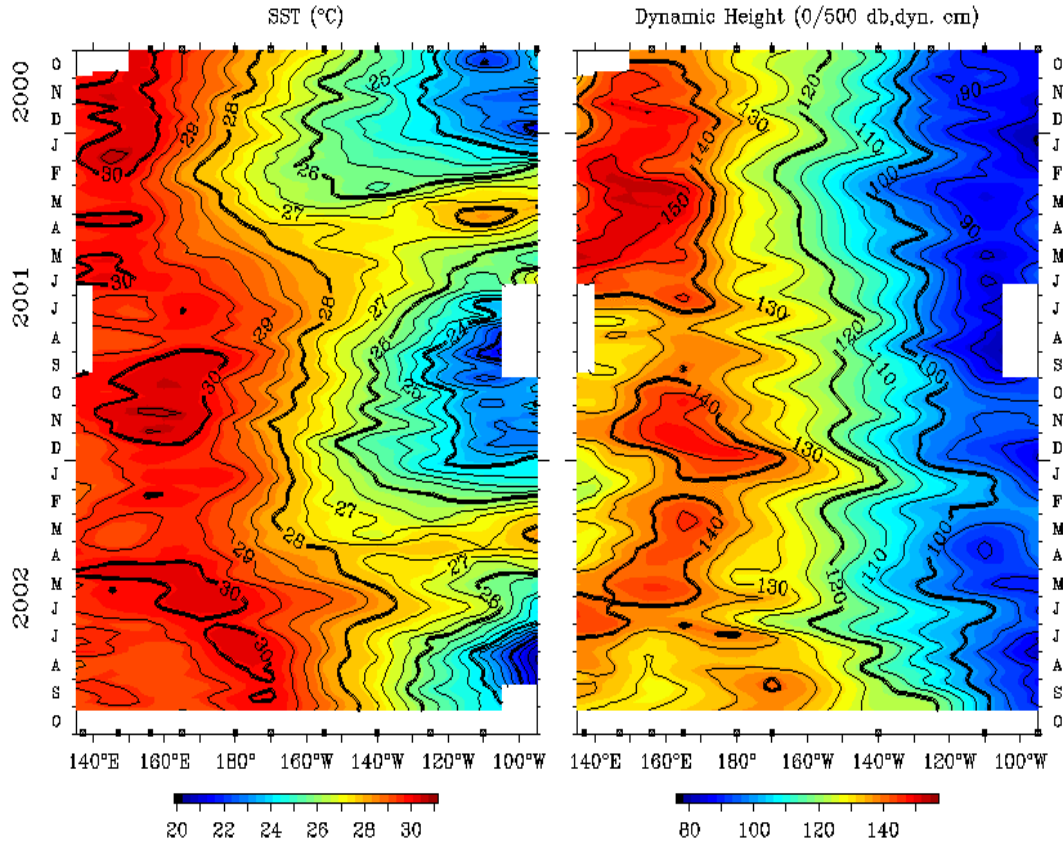


All of the blue dots represent surface moorings with atmospheric boundary layer and subsurface temperature and velocity measurement. On selected locations on the equator, moored ADCP (acoustic Doppler current profilers) collect current profiles in the upper ocean. All of the data are telemetered back and can be accessed in ‘realtime’. For example, one can see the wind anomalies from the mean seasonal cycle and SST (sea surface temperature) from 8 October 2002 (below). Winds are blowing towards a SST maximum in the western tropical Pacific and cold SSTs can be seen in the east. This is close to the “normal” condition since the anomalies are weak.



Other data can be seen showing the changes in SST and in surface dynamic height on the equator, the latter coming from the moorings.

Five-Day SST and Dynamic Height 2°S to 2°N Average

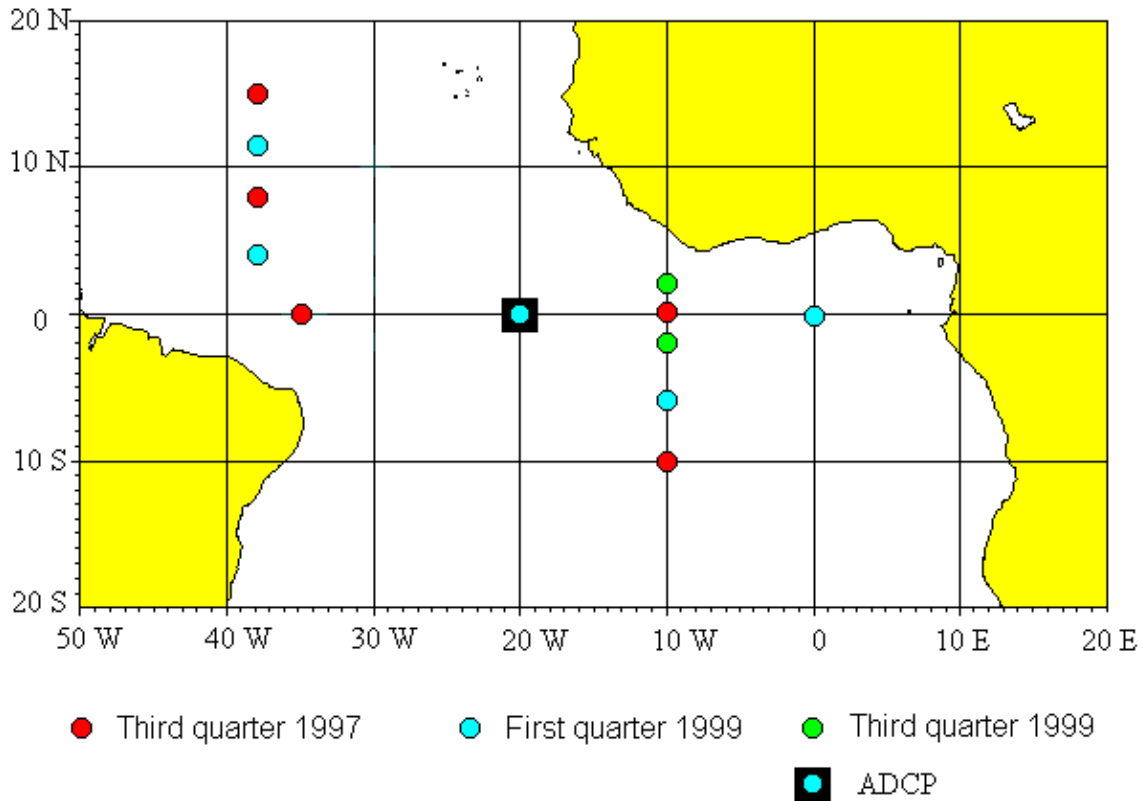


TAO Project Office/PMEL/NOAA

Oct 9 2002

In addition to the seasonal cycle of SST on the left, one can see interannual changes in the dynamic topography at the sea surface (relative to 500 db) showing a large reduction in the sea surface height across the Pacific between, say, March 2001 and Sept. 2002.

A similar but less extensive array is in place in the tropical Atlantic, called PIRATA (<http://www.pmel.noaa.gov/pirata/images/pirata.gif>). The mooring array is shown next.



Data are somewhat more difficult to access, and often have “gaps” due to mooring failure or damage from vandalism. The array is still considered a “pilot” array, and there are ongoing discussions to make additions/changes. But compared to the rest of the ocean, the Pacific and Atlantic tropics are in MUCH better condition for data availability from *in situ* instrumentation.